

Nathan Phillips · Barbara J. Bond · Michael G. Ryan

Gas exchange and hydraulic properties in the crowns of two tree species in a Panamanian moist forest

Received: 2 August 1999 / Accepted: 3 October 2000 / Published online: 7 December 2000
© Springer-Verlag 2000

Abstract Hydraulic properties and gas exchange were measured in branches of two tropical tree species (*Simarouba amara* Aubl. and *Tapirira guianensis* Aubl.) in a moist lowland forest in Panama. Branch-level sapflow, leaf-level stomatal conductance, and water potential measurements, along with measurements of specific hydraulic conductivity of stems in crown tops, were used to relate hydraulic parameters to leaf conductance in two individuals of each species. Branches of the taller trees for each species (28 m, 31 m) showed much higher leaf-specific hydraulic conductance and leaf vapor-phase conductance than those of the smaller trees (18m, 23m). This was probably related to the leaf-to-sapwood area ratio in branches of taller trees, which was less than half that in branches of smaller trees. Dye staining showed evidence of massive cavitation in all trees, indicating that stomata do not control leaf water potential to prevent xylem cavitation in these species. Stomatal conductance of intact leaves also appeared to be insensitive to leaf area removal treatment of nearby foliage. Nevertheless, a simple mass-balance model of water flux combining hydraulic and vapor transport was in close agreement with observed maximal vapor-phase conductance in the four trees ($r^2=0.98$, $P=0.006$). Our results suggest that the major organismal control over water flux in these species is by structural (leaf area) rather than physiological (stomatal) means.

Keywords Cavitation · Hydraulics · Stomata · Tropical forest · Xylem

List of symbols A_L : one-sided leaf area (m^2) · A_S : sapwood area (cm^2) · $A_L:A_S$: leaf-to-sapwood area ratio ($m^2 cm^{-2}$) · c_p : specific heat of air at constant pressure ($J kg^{-1} °C^{-1}$) · D : foliage-to-bulk air vapor pressure difference (kPa) · D_a : air vapor pressure deficit (kPa) · E : branch transpiration ($mmol m^{-2} s^{-1}$) · F : flux of water ($g s^{-1}$) · g : acceleration due to gravity ($kg m^{-2} s^{-1}$) · g_L : leaf conductance ($mmol m^{-2} s^{-1}$) · g_s : stomatal conductance ($mmol m^{-2} s^{-1}$) · h : height of tree (m) · J_S : sap flux per unit sapwood area ($g m^{-2} s^{-1}$) · k : saturated sapwood permeability (m^{-2}) · K_L : leaf specific hydraulic conductance ($kg m^{-1} s^{-1} MPa^{-1}$) · k_S : sapwood specific hydraulic conductivity ($kg m^{-1} s^{-1} MPa^{-1}$) · l : length of branch segment (m) · P : atmospheric pressure (kPa) · Q_p : photosynthetic photon flux density ($\mu mol m^{-2} s^{-1}$) · T_L : leaf temperature ($°C$) · γ : psychrometric constant ($kPa °C^{-1}$) · λ : latent heat of vaporization of water ($J kg^{-1}$) · η : viscosity of water ($Ns m^{-2}$) · ρ_a : density of air ($kg m^{-3}$) · ρ_w : density of water ($kg m^{-3}$) · Ψ_L : leaf water potential (MPa) · Ψ_S : soil water potential (MPa) · Ω : aerodynamic coupling coefficient

N. Phillips (✉)
Geography Department, Boston University,
675 Commonwealth Ave., Boston, MA 02215, USA
e-mail: nathan@bu.edu

B.J. Bond
Forest Science Department, Oregon State University, Corvallis,
OR 97331, USA

M.G. Ryan
US Forest Service, Rocky Mountain Research Station,
240 W. Prospect Road, Fort Collins, CO 80526, USA,
and Graduate Degree Program in Ecology,
Colorado State University, Fort Collins, Colorado 80523, USA

Introduction

Recently, hydraulic properties of trees have been suggested to limit height and biomass growth in old trees and forests (Yoder et al. 1994; Ryan and Yoder 1997). Features associated with tree hydraulic architecture that could influence its gas exchange include tree height and hydraulic path length, leaf and sapwood areas, sapwood specific conductivity, stomatal conductance, leaf and crown boundary layer conductance, and leaf-to-soil water potential difference. An essential sign of hydraulic limitation to gas exchange in trees is stomata closure of leaves under water stress. In this study, we examined the crowns of four tropical trees of two species to investigate

the dependence of gas exchange on leaf water status and hydraulic properties.

Although stomatal control may help trees with a relatively fixed hydraulic architecture to *endure* decreases in hydraulic conductance, such as caused by hydraulic path-length increase with tree growth, changes in tree hydraulic architecture with tree size may possibly serve to *avoid* a decrease in hydraulic conductance. For example, Pothier et al. (1989) showed that xylem anatomy changed with tree age so as to increase sapwood permeability. This anatomical change would tend to offset decreases in whole-tree conductance caused by increased path length. Another mechanism for avoiding hydraulic constraints on leaf-gas exchange may be decreased allocation of growth resources to foliage relative to sapwood. In response to seasonal drought, decreases in allocation to foliage can occur by either partial or complete leaf shedding. Decreases in leaf-to-sapwood area ratio ($A_L:A_S$) could also be expected to occur on a long-term basis associated with the increased path length as a tree grows in height.

A formal representation of this allocation pattern was provided by Whitehead et al. (1984), who used conservation of mass flux to link the liquid flux of water within trees to the vapor flux of water leaving canopies:

$$\frac{A_L}{A_S} = \frac{k \langle \Delta\Psi \rangle c_p \lambda \gamma \rho_w}{D_a h \langle g_s \rangle \eta \rho_a} \quad (1)$$

where A_L is one-sided leaf area, A_S is sapwood area, k is saturated sapwood permeability, D_a is air vapor pressure deficit, h is tree height, g_s is stomatal conductance, c_p is specific heat of air at constant pressure, λ is latent heat of vaporization of water, γ is the psychrometric constant, ρ_w is the density of water, η is the viscosity of water, and ρ_a is the density of air. The brackets ($\langle \rangle$) indicate averaging over the crown, weighted by the physiological activities of different positions within the crown, and $\Delta\Psi = \Psi_L - \Psi_S - \rho_w g h$, where Ψ_L is leaf water potential, Ψ_S is soil water potential, g is the acceleration due to gravity, and h is mean canopy height.

This expression is strictly applicable only to well-ventilated canopies during steady-state conditions and does not account for root membrane conductance or feedbacks between $\Delta\Psi$ and saturated sapwood permeability (k) through cavitation. Nevertheless, it illustrates generally the inverse dependency of $A_L:A_S$ on hydraulic path length, and the possibility that an increased stomatal conductance over the crown ($\langle g_s \rangle$) could result from decrease in $A_L:A_S$. Such an effect has been demonstrated artificially by reducing leaf area in larger trees, which resulted in a stomatal conductance more similar to that of smaller trees (Hubbard et al. 1999).

In this study, we examined the coordination between stomata, leaf water potential and branch hydraulic properties. Specifically, we addressed the questions: Do stomata close before cavitation occurs in the branches of these species? Does a change in branch $A_L:A_S$ affect an inverse response in g_s ? By removing a portion of the leaves in selected branches, we could address this ques-

tion as the inverse relationship in the Whitehead model suggests. By choosing a short and tall individual from each species we “bracketed” the species across a wide range of mature tree size, whilst recognizing the limitations of this sampling approach for making general inferences regarding tree height.

Materials and methods

Site description

This study was carried out during the dry season, February 1998, at the Smithsonian Tropical Research Institute’s (STRI) Fort Sherman canopy crane site in a moist lowland tropical forest in Panama. The site, located near the Caribbean entrance to the Panama canal, receives an average of 3.4 m of rain annually. However, atmospheric conditions previous to and during our study were unusually dry because of a severe El Niño weather pattern. Nevertheless, we found indications that Ψ_S was constant and near zero because the site soils continuously seeped moisture over the duration of our study. Soils at the site occur on Chagres sandstone bedrock and are unclassified but of clayey texture. The forest canopy reached about 35 m from the ground.

Species

Four individuals, two from each of the two species *Simarouba amara* Aubl. (Simaroubaceae) and *Tapirira guianensis* Aubl. (Anacardiaceae), were used for measurements. The individuals from these species were selected because all four trees were either dominant or located in canopy gaps with high light exposure. *S. amara* is a fast-growing pioneer species (Oberbauer et al. 1993) abundant in high-light areas, but may also persist in shade conditions. Less is known about *T. guianensis*, but it has the distinction of being a shade-tolerant, wet-forest indicator species (R. Condit, STRI, personal communication). Both species are evergreen but display some seasonal shifts in leaf turnover (S.J. Wright, STRI, personal communication). *S. amara* displayed its highest leaf turnover of the year around the period of our study, but total leaf area remains fairly constant year round. *T. guianensis* showed rapid pulses of new leaf growth between September and October and again in January, and then a slow decline in leaf number throughout the rest of the year from loss of single leaves.

Vascular anatomy

Four upper-canopy, exposed branches on each tree were selected for detailed measurements. Exposed, upper canopy branches were chosen because they represented the most physiologically-active portions of the crown and allowed between-tree comparison. Table 1 contains tree and branch dimensions. Two of the four branches on each tree (eight total branches) were used for biomass and hydraulic measurements. Cut ends of harvested branches were immediately covered with saturated cloths and placed in plastic bags for transport to a laboratory refrigerator (maintained at approximately 5°C). Cross-sectional samples of stemwood from the eight harvested branches were used to examine sapwood anatomy. Four 20- μ m-thick xylem cross-sectional samples from each of the eight harvested branches were sectioned with a sliding microtome and fixed on glass slides with a 70% ethyl alcohol solution. Vessel lumen areas were determined by using a digital imaging and analysis system (Sony CCD/RGB Color Video Camera installed on a Nikon Labophot-2 compound microscope, with a NIH Image v. 1.59 public domain-image processing and analysis program). Four sub-samples were imaged for each stem cross-section. Vessel diameter and area histograms were constructed for each sample, as well as vessel number density on a cross-sectional xylem-area basis.

Table 1 Structural characteristics of trees and branches in this study. Branch diameters are at the positions of sapflow sensors and leaf areas are distal to sapflow sensors (standard errors in parentheses)

ID No.	<i>Simarouba amara</i>		<i>Tapirira guianensis</i>	
	40688	36931	39060	36627
Tree height (m)	18	31	23	28
Stem diameter at 1.3 m (m)	0.14	0.56	0.26	0.64
Branch diameter ($n=4$) (mm)	14 (0.4)	15 (0.4)	13 (0.6)	14 (0.3)
Branch distal leaf area ($n=4$) (m ²)	0.91 (0.29)	0.44 (0.12)	1.24 (0.40)	0.39 (0.06)

Vessel density and the distribution of vessel sizes throughout the sapwood of branches were used to estimate maximal branch sapwood specific hydraulic conductivity (k_S) (that is, neglecting cavitation) according to Poiseuille's law:

$$k_S = \frac{\sum \frac{\pi r^4}{8\eta}}{A_S} \quad (2)$$

where r is the radius of a circle having the same area as the corresponding vessel, η is the viscosity of water, and A_S is sapwood area. This calculation neglects any restrictions on vessel ends or other deviations from Poiseuille's law. Summations were performed over each of the four sub-samples from each branch. Branch sub-samples were pooled for branches of the same tree after verifying that sub-sample means were not significantly different ($P > 0.1$).

Hydraulic conductivity

Native cavitation in first and second order stems from the eight harvested branches was assessed by examining the extent of dye perfusion (0.22 μm filtered, 0.05% safranin dye) through branches supplied from cut ends located about 10 cm upstream from the inspected cross-section. The cut branches were second to fourth order, and smaller stems cut under water from these branches (typically 0.5–1.5 cm in diameter) were used for specific conductivity measurements. Stained and total sapwood areas were determined using the imaging-analysis system described above. All measurements of specific conductivity were made within 3–5 days after branches were harvested.

Native specific conductivity measurements were made by supplying cut stem segments with 0.22 μm filtered water at a gravitational pressure potential of 10 kPa. An apparatus was used consisting of pipettes and tygon tubing which provided a constant 1-m gravitational head to branches and the ability to visually determine flow rate by timing meniscus movement in a graduated pipette. Tygon tubing was connected and sealed to branch segments with Parafilm. Segment lengths and small-end diameters were measured, and steady-state volumetric flux rates recorded, on 28 samples distributed roughly evenly among branches from the four trees. Specific conductivity (k_S) was computed as

$$k_S = \frac{Fl}{pA_S} \quad (3)$$

where F = flux, l = segment length, and p = pressure gradient.

On selected stem segments used for measuring k_S , cavitation vulnerability was also estimated using a gas-pressurizing collar placed and sealed around the stem segment (PMS Instruments, Corvallis, Ore.). Gas pressure (nitrogen) was applied for several minutes at 0.25 MPa increments through a maximal pressure of 2.0 MPa. After each increase in gas pressure, stems were left alone for several minutes before k_S was estimated using the method described above.

Branch-level measurements

Measurements of sap flow were made on each of the four branches of each tree by using sap-flow probes described by Granier (1987). The probes were 10-mm long and dissipated 100 mW into branch sapwood. Temperature differences were recorded between

thermojunctions located in the center of the heated probes and reference thermojunctions located about 10 cm upstream. To minimize ambient temperature gradients within the branches, we insulated them with plumbing pipe insulation and silicon sealant and covered them with reflective bubble wrap. Stable night-time and early morning temperature differences indicated that ambient temperature gradients were negligible. Sap-flux density (J_S ; $\text{g}_{\text{H}_2\text{O}} \text{m}^{-2} \text{xylem} \text{s}^{-1}$) was estimated from temperature differences using an empirical calibration (Granier 1987). This calibration was originally performed for 20 mm long sensors but was assumed here to apply to 10 mm sensors in smaller branches than those used by Granier. Branch transpiration (E ; $\text{mmol m}^{-2} \text{s}^{-1}$) was estimated by multiplying J_S by the cross-sectional sapwood area (A_S) at the position of the heated sensor and dividing by distal one-sided leaf area (A_L). Sapwood areas, determined by subsequent harvesting and inspection with a microscope, were found to be nearly 100% of the area inside bark.

Data loggers (Campbell Scientific, Logan, Utah) were placed at the bottom of each of the four trees and connected to signal cables from branch sap-flow probes. Temperature differences were measured every 30 s and averaged and recorded every 5 min. Data logging commenced at 12:00 16 February on all 16 branches (four branches from each of the four trees).

Leaf area removal treatments

The experimentation on the 16 branches proceeded in two steps. First, on the morning of 20 February, leaf area removal (LAR) treatments were performed on two branches of each tree before any harvesting, with about 50% of leaf area removed from branches. Removed leaves were saved for computing area and developing a relationship between leaf count and area that could be applied to non-harvested foliage for estimating leaf area. Second, two of the four branches from each tree (one with LAR treatment, one without) were harvested on the afternoon of 21 February; sap-flow measurements continued on the remaining eight branches (so that one branch with LAR treatment and one without also remained).

Leaf-level measurements

Photosynthetically active radiation (Q_p ; $\mu\text{mol m}^{-2} \text{s}^{-1}$) was measured on the foliage of each of the 16 branches for as long as they were on the tree with photo-diode sensors (LI190SA, LI-COR, Lincoln, Neb.) connected with current-to-voltage adapters (Phillips and Bond 1999) to miniature data loggers (HOB0 H8, Onset Computer Corp., Pocasset, Mass.). Foliage temperatures (T_L ; $^{\circ}\text{C}$) were measured with a 2-mm diameter thermistor taped to the abaxial side of a representative leaf on each branch. The thickness of the thermistor allowed space for stomatal exchange directly above and around the thermistor. Both Q_p and T_L were logged at 5-min intervals with the miniature data loggers. Foliage-to-bulk air vapor pressure difference (D ; kPa) for each branch was computed as the difference between saturation vapor pressure at leaf temperature and ambient vapor pressure obtained from air temperature and relative humidity recorded on the crane tower. Branch leaf conductance (g_L ; $\text{mmol m}^{-2} \text{s}^{-1}$) was computed as

$$g_L = \frac{EP}{D} \quad (4)$$

where E is branch transpiration and P is atmospheric pressure. This estimate of g_L included atmospheric conductance from the leaf level to the point of ambient vapor pressure measurement near the crane boom.

In addition to branch g_L scaled from sap-flow measurements, diurnal measurements of leaf-level stomatal conductance (g_s) were made on leaves using a portable photosynthesis system (LI-6400; LI-COR, Lincoln, Neb.) in order to assess the effect of branch boundary layer conductance on g_L . Measurements were made in full sun and at ambient temperature. Relative humidity was maintained at approximately 65%, less than ambient values (mid-day averages 80–90%), in order to improve accuracy of vapor flux rate measurements.

In order to detect variation among trees in branch aerodynamic boundary-layer conductance, an aerodynamic coupling coefficient (Ω , Jarvis and McNaughton 1986) was computed for each branch according to Martin (1989), by using $1/g_s$ and $1/g_L$ in a resistance subtraction method (see Meinzer et al. 1997).

Diurnal courses of leaf water potential (Ψ_L) were measured with a Scholander-type pressure chamber (PMS, Corvallis, Ore.). One predawn set of Ψ_L measurements was made on 20 February. Intact shoots had been covered with reflective paper bags for at least 24 h prior to measurement to induce stomatal closure and promote an equilibrium between leaf water potential (Ψ_L) and xylem water potential. From predawn to dawn on 20 February, 3–4 measurements of Ψ_L were made on foliage from the selected branches, on both bagged and unbagged shoots.

Estimates of leaf specific hydraulic conductance (K_L) in the soil-to-branch foliage pathway were computed as

$$K_L = \frac{Eh}{\Delta\Psi} \quad (5)$$

where E is transpiration rate, h is tree height, and $\Delta\Psi$ is the difference between measured Ψ_L and an estimate of Ψ_S by using gravity-corrected predawn values of Ψ_L ($\Psi_L - \Psi_S - \rho_w gh$). Replicate estimates of K_L on the same tree were separated in time by several hours to days.

Results

Branch sapwood- and leaf-specific conductivity

In all branches, vessel sizes ranged from ca. 20 to 90 μm , and vessel density was 30–80 mm^{-2} . Vessel size distributions and density were used to compute a maximal theoret-

ical k_S from Poiseuille's law. All values of this maximal k_S fell in the range of 2–10 $\text{kg m}^{-1} \text{s}^{-1} \text{MPa}^{-1}$ (Table 2), which is within the range typical for tropical tree branches with diameters similar to those in this study (Tyree and Ewers 1996). For all branches from all trees, values of native k_S obtained from excised branch segments were less than the maximal theoretical values calculated from Poiseuille's law (Table 2). This reduction from maximal theoretical values was likely caused by a combination of native cavitation and departures from ideal Poiseuille flow due to vessel constrictions or wall roughness. An indication of the degree of cavitation was given by the results from dye perfusions. The percentages of dyed to total sapwood areas averaged only 39% and 36% for branch samples from the short and tall *S. amara*, and 41% and 27% for the short and tall *T. guianensis*, respectively. There did not appear to be systematic radial or circumferential trends in the spatial distribution of stained areas. Instead, distinct clumps of unstained areas in the order of a few mm^2 appeared to be distributed over the sapwood cross-sections. Values of native k_S remained within the range reported previously for tropical trees (Tyree and Ewers 1996).

Plots of cavitation vulnerability showed large decreases in k_S at relatively mild applied gas pressures in branches from all of the trees (Fig. 1a, b). We were able to successfully perform these vulnerability estimates on three branches from the 18-m *Simarouba* tree, two branches from each of the 31-m *Simarouba* and 23-m *Tapirira*, and only a single branch of the 28-m *Tapirira*. Compared with temperate species, the vulnerability curves appear similar to those in *Populus deltoides*, a species considered to be highly vulnerable to drought-induced cavitation (Tyree and Ewers 1996).

Leaf and sapwood areas

The taller tree of each species had an $A_L:A_S$ about one-third that of the shorter individual (Table 2). Values of

Table 2 Results from branch hydraulic measurements (standard errors in parentheses)

	<i>Simarouba amara</i>		<i>Tapirira guianensis</i>	
Height (m)	18	31	23	28
Vessel density (# mm^{-2})	50	49	28	75
$A_L:A_S$ (m^2cm^{-2})	0.71 (0.16)	0.27 (0.06)	0.99 (0.09)	0.30 (0.03)
g_L (maximal) ($\text{mmol m}^{-2} \text{s}^{-1}$)	70	160	100	700
g_s (midday) ($\text{mmol m}^{-2} \text{s}^{-1}$)	220 (20)	250 (20)	100 (10)	190 (20)
k_S (maximal) ($\text{kg m}^{-1} \text{s}^{-1} \text{MPa}^{-1}$)	2.2 (0.3)	2.9 (0.5)	7.8 (0.9)	6.3 (1.3)
Percent non-conductive sapwood	61	64	59	73
K_L ($\text{kg m}^{-1} \text{s}^{-1} \text{MPa}^{-1}$)	0.10 (0.02)	0.30 (0.02)	0.20 (0.03)	0.32 (0.05)
Ψ_L (midday) (MPa)	-1.16 (0.6)	-1.25 (0.6)	-0.93 (0.7)	-1.32 (0.8)

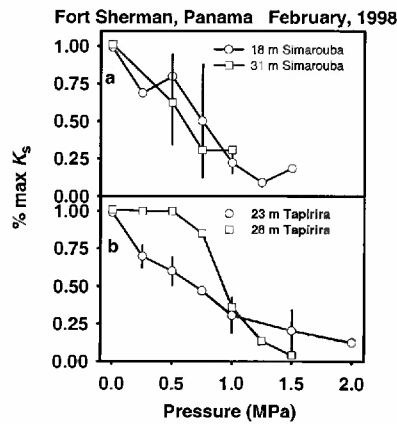


Fig. 1 Percent loss of native specific hydraulic conductivity (k_s) with applied gas pressure for **a** *Simarouba amara* and **b** *Tapirira guianensis*

$A_L:A_S$ ranged from $0.27 \text{ m}^2 \text{ cm}^{-2}$ to $0.99 \text{ m}^2 \text{ cm}^{-2}$, which is within the range typical for tropical tree branches of the same diameter (Tyree and Ewers 1996).

Leaf water potentials

Midday leaf water potentials (Ψ_L) averaged between -0.9 and -1.3 MPa in branch foliage from all trees (Table 2), and the effect of gravity and path length on Ψ_L was not significant ($P = 0.4$). Predawn measurements of Ψ_L for bagged and unbagged shoots did not differ ($P = 0.5$), nor did they differ appreciably from the gravitational $\Delta\Psi$ alone.

Sapflow and vapor-phase conductance

Meteorological conditions and sapflow per unit sapwood and leaf areas for the 11 days of this study are presented in Fig. 2. Vapor pressure deficit of the canopy air stayed below 1 kPa throughout the study, while photosynthetically-active radiation peaked at about $2 \text{ mmol m}^{-2} \text{ s}^{-1}$ with scattered clouds during most days (Fig. 2a) and two trace rain events (not shown). Sap flux per unit sapwood area (J_s) and per unit leaf area (E) were relatively constant throughout the 11 days (Fig. 2b–e), with the exception of the 18-m *Simarouba* (Fig. 2b), which showed a decline in J_s and E after the first 4 days of the time course. The J_s in branches of small versus large trees (Fig. 3a, b) showed a similar relationship in both *S. amara* and *T. guianensis*. Small trees had slightly lower J_s than large trees in both species, and *T. guianensis* had values of J_s ca. 1.5 times those of *S. amara*. Although stem hydraulic capacitance is an important element in the hydraulic function of trees that could have affected these relationships (Goldstein et al. 1998), it was not a subject of detailed measurements in this study. However, we assessed whether stem capacitance played a significant role in branch fluxes by comparing diurnal dynam-

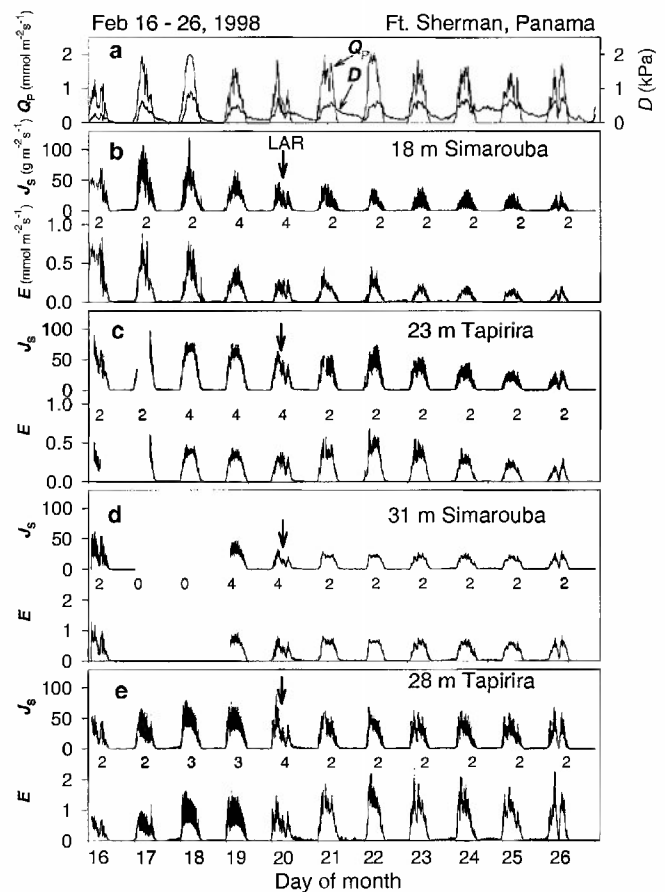


Fig. 2 **a** Meteorological conditions. Air vapor pressure deficit (D) and overstory photosynthetically-active radiation (Q_p). **b** Branch water flux per unit sapwood and leaf area (upper and lower traces, respectively) in the 18-m tall *Simarouba* tree. **c** Branch water flux per unit sapwood and leaf area (upper and lower traces, respectively) in the 23-m tall *Tapirira* tree. Flux units are the same as in **a**. **d** Branch water flux per unit sapwood and leaf area (upper and lower traces, respectively) in the 31-m tall *Simarouba* tree. Flux units are the same as in **a**. **e** Branch water flux per unit sapwood and leaf area (upper and lower traces, respectively) in the 28-m tall *Tapirira* tree. Flux units are the same as in **a**. Numbers between traces are the number of branches averaged in the traces (standard errors shown). Downward arrow in panels indicates when the leaf area reduction treatment was performed

ics of branch fluxes in trees of different sizes. If stem capacitance were important, we would expect to find that branches of larger trees showed pronounced peaks in morning sapflow relative to afternoon flux (Goldstein et al. 1998). To the extent that stem capacitance alters the diurnal shape of branch sap flow, the nearly linear relationship between J_s in small and large trees suggests that capacitance played at most a minor role in helping to alleviate hydraulic constraints in large trees compared with small trees, or at least a similar role in both. Furthermore, when an index of whole tree conductance was computed as $J_s \cdot h / (\Psi_L - \Psi_S - \rho_w g h)$, and plotted against time of day, no significant relationship resulted, though a relationship would have been expected with stem capacitance (data not shown).

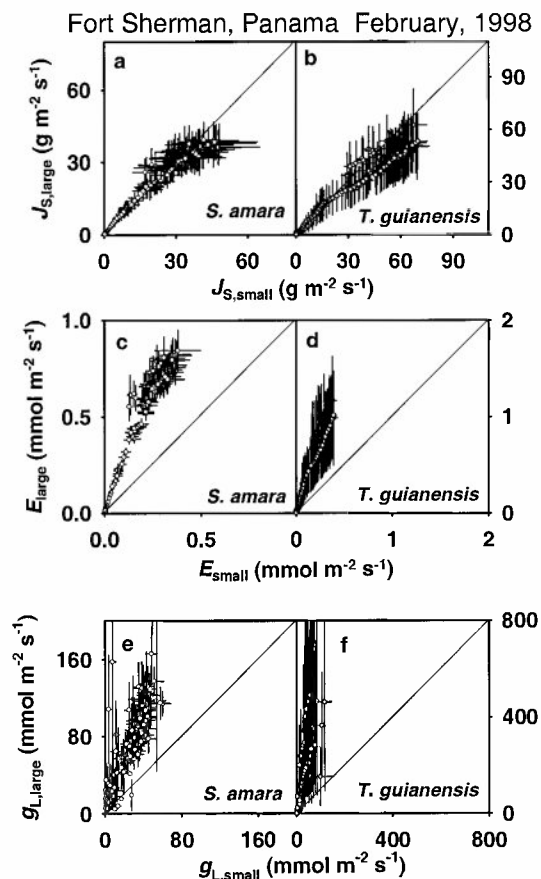


Fig. 3 Relationships between water flux per unit sapwood area (J_s ; a,b), per unit leaf area (E ; c,d) and leaf conductance (g_L ; e,f) between large trees (31-m *Simarouba amara*; 28-m *Tapirira guianensis*) and small trees (18-m *Simarouba amara*; 23-m *Tapirira guianensis*). The 1:1 line is shown in each panel

Branches from small trees in both species had much higher $A_L:A_S$ than branches from large trees (Table 2). Therefore, when J_s was expressed per unit leaf area to estimate E , the E of large trees averaged about twice the rate of E from small trees (Fig. 3c, d). Differences between branches of small and large trees diverged even further in their values of g_L (Fig. 3e, f). Maximal values of g_L reached only ca. $160\ mmol\ m^{-2}\ s^{-1}$ in branches of the large *S. amara*, but ca. $800\ mmol\ m^{-2}\ s^{-1}$ in branches of the large *T. guianensis*. These maximal values were within the range Lloyd et al. (1995) found using meteorological methods for an Amazonian rain forest. Although these values of g_L included a boundary layer, Ω (our aerodynamic coupling coefficient) was ca. 0.7–0.8 for all branches, indicating relatively de-coupled branches, and did not differ between branches from small and large trees ($P > 0.05$). Average midday values of g_s measured with a gas-exchange system in foliage of large trees were also equal to or higher than those in small trees (Table 2). The treatment to reduce leaf area did not appear to substantially increase g_L in three branches for which we had pre- and post-LAR data (Fig. 4a, c, d; the

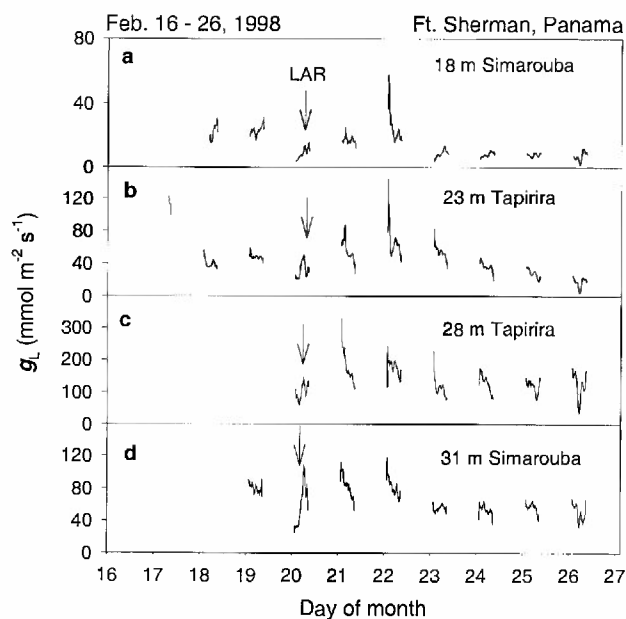


Fig. 4 Time series of leaf conductance (g_L) derived from sapflow and leaf-to-air vapor pressure difference (D) for the a 18-m *Simarouba*, b 23-m *Tapirira*, c 28-m *Tapirira*, d 31-m *Simarouba*. The leaf area removal treatment on 20 February is indicated by the downward arrows

branch from the 28-m *Tapirira* (Fig. 4c) did not have pre-LAR data because of instrument problems.

In spite of our attempts to choose equally sunlit branches from all trees, daylight averaged Q_P (from 10:00 to 16:00) was substantially higher in taller trees ($321, 324, 802, 777\ \mu mol\ m^{-2}\ s^{-1}$ in the 18-m *Simarouba*, 23-m *Tapirira*, 28-m *Tapirira*, 31-m *Simarouba*, respectively). Nevertheless, g_s showed no relationship to instantaneous Q_P in any of the branches (data not shown). Furthermore, daylight-averaged Q_P did not explain variation in midday averaged g_s in each tree. It is possible that the instantaneous sampling of Q_P every 5 min was not sufficient to adequately characterize the average light conditions, either for each 5-min period or for a daily average.

Discussion

Several studies have demonstrated sensitivity of stomata to changes in plant leaf-specific hydraulic conductance in both temperate plants (Teskey et al. 1983; Sperry and Pockman 1993; Sperry et al. 1993; Whitehead et al. 1996; Pataki et al. 1998) and a tropical crop (Meinzer and Grantz 1990). In five tropical tree species, Andrade et al. (1998) observed a saturating relationship of stomatal and crown conductance to whole tree leaf-specific hydraulic conductance. Inconsistent with the findings from those studies was our lack of an observation of a clear stomatal response to a change in leaf specific hydraulic conductivity through the LAR treatment (Fig. 4). Fur-

thermore, the massive cavitation we observed in branches (Table 2) indicates that stomata do not close in these species before such extensive cavitation occurs. Even if xylem water potential were substantially less negative than typical mid-day Ψ_L (Table 2), Fig. 1 indicates that significant cavitation may be expected to occur in these species. If these were unusually high levels of cavitation for these species due to the extended El Niño period during our study, this must have been because of atmospheric drought and its effects on above-ground hydraulic desiccation, rather than a soil moisture deficit, as we observed the soil to continuously seep water from banks.

To better interpret the functional consequences of cavitation observed in this study, more information is needed about potential trade-offs related to cavitation in these trees. Although it is usually assumed that cavitation is deleterious to plant function, Sperry (1995) has discussed potential advantages of cavitation, including the provision of water from cavitated xylem conduits that may buffer leaf water status (Dixon et al. 1984; Lo Gullo and Salleo 1992). In fact, the most negative Ψ_L in this study (-1.3 MPa) is relatively moderate and did not appear to cause stomatal closure. Furthermore, if these trees remove embolisms diurnally as was found by Zwieniecki and Holbrook (1998), our afternoon harvesting of branches might represent a minimal or highly variable k_S , and not an effective k_S under which stomata operate.

Beyond the physiological consequences of the cavitation observed in this study are technical implications for the use of Granier sap flow sensors in embolized xylem. Clearwater et al. (1999) have shown that errors in estimated sap flux rates may be incurred when portions of the sap flow probe sample non-conducting xylem. While our microscopic inspections of the cross sections in which sap flow probes were inserted showed that they were nearly 100% sapwood, it is likely that portions of this sapwood were non-functional, given the evidence of substantial cavitation from our subsequent dye perfusions through other stem segments. However, we did not assess the particular distributions of cavitated zones in the region of each sap flow sensor, and are thus unable to make a correction for this effect. If diel cavitation reversal as found by Zwieniecki and Holbrook (1998) is common, then the issue raised by Clearwater et al. (1999) will need to be extended to a consideration of probe function in dynamically variable sapwood area.

While it could be expected that trees with larger hydraulic path length would show a greater increase in g_S or g_L with LAR treatment, such treatment did not appear to substantially increase g_L in any of the trees (Fig. 4). Since diel variation in g_L was large to begin with (Fig. 4), it is difficult to detect a clear response to LAR. There may have been a short-term increase in g_L in the 2 days following the LAR treatment (Fig. 4); but there is no clear indication of an increase in g_L over the following days. It is possible that the absence of a response in the 31-m *Simarouba* tree was due to the decrease in $A_L:A_S$ in branches of large trees (Table 2), which resulted in a natural LAR "treatment".

The only observation in this study consistent with a possible hydraulic constraint to gas exchange in these branches is the reduced $A_L:A_S$ in the taller trees of each species. While we cannot generalize from the limited information from this study, if such a pattern persisted with further replication, it may indicate an adjustment to increase hydraulic sufficiency with increased tree height, consistent with the Whitehead model. An interspecific survey of $A_L:A_S$ and tree size indicates, with some exceptions, a widespread response (McDowell et al., to be published).

From our data, it is not possible to assess whether the higher g_L in larger trees can be attributed solely to a reduced $A_L:A_S$ or to the fact that branches from taller trees experienced higher average light conditions. The lack of a relationship between g_S and either instantaneous or daily averaged Q_P in branches from all trees at least suggests a lack of a strong light limitation in the smaller trees. In any case, the higher g_L in taller trees combined with the extensive cavitation in branches from all trees indicate clearly that stomata in these species do not close due to hydraulic constraints.

It is also possible that a higher proportion of foliage was shaded in smaller trees because of lower light conditions. If so, our measurements of leaf temperature on leaves of exposed branches could overestimate the branch level vapor pressure difference that drives flux in branches from smaller trees. In such a case, we would have overestimated g_L in branches of smaller trees, and the difference between g_L in branches of smaller and taller trees would be even higher. Thus, this possible bias introduced by our leaf temperature measurements would reinforce our conclusion that branches of larger trees show higher g_L .

The mass balance model of water flux in trees proposed by Whitehead et al. (1984) illustrates how both physiological and structural features of trees may interact to control their water flux. For comparison with vapor phase flux predicted from the Whitehead model, we predicted g_L in two ways: by using measured sapwood specific hydraulic conductivity (k_S) that included effects of cavitation, and by using "saturated" k_S , predicted from Poiseuille's law, together with anatomical measurements. Predictions of g_L in each branch were made by re-arranging equation (1), for both native k and maximum k predicted from Poiseuille's law, and using average midday values of D and gravity-corrected leaf-to-soil $\Delta\Psi$. Thus, this model formulation equates water flux in trees to total vapor-phase conductance, rather than stomatal conductance alone and is, therefore, an extended version of the Whitehead model, similar to that shown in Sperry (1995, Eq. 5). The predicted values of g_L among branches in a tree were compared with observed values. Here we assumed that k of branches could be used as a measure of whole-tree average k , which we recognize as a tenuous assumption (Whitehead and Hinckley 1991). Even so, contrary to our expectation, g_L based on measured k_S was not even correlated with average g_L , ($P = 0.6$; data not shown). However, a comparison of ob-

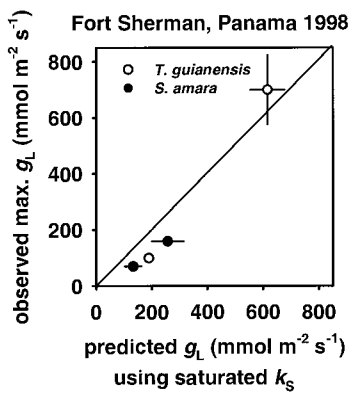


Fig. 5 Observed versus predicted maximal branch leaf conductance (g_L). Predicted g_L was based on maximal specific hydraulic conductivity (k_S) predicted from Poiseuille's law

served maximal g_L based on “saturated” k_S versus that predicted from the hydraulic-vapor flux model appeared to show good agreement (Fig. 5). Thus, at least in these individuals from the two species studied, stomata appeared to be “tuned” to potential hydraulic sufficiency rather than to actual hydraulic sufficiency. It is quite interesting to note the agreement between “saturated” k_S predicted here from Poiseuille's law and the Whitehead model, which similarly uses a saturated permeability. An interesting extension of the Whitehead model would be to include the variability in k_S derived from cavitation vulnerability curves, thereby including a functional, if indirect, relationship between k_S and Ψ_L into the mass balance equation.

Acknowledgements We thank Edwin Andrade, Rick Condit, Jose Herrera, Steve Paton, Robert Pearcy, Myrna Samaniego, Rachel Spicer, and Joe Wright for assistance. This project was funded through the US Department of Agriculture NRI Competitive Grants Program, contract number 97–35101–4318.

References

- Andrade JL, Meinzer FC, Goldstein G, Holbrook NM, Cavelier J, Jackson P, Silveira K (1998) Regulation of water flux through trunks, branches, and leaves in trees of a lowland tropical forest. *Oecologia* 115:463–471
- Clearwater MJ, Meinzer FC, Andrade JL, Goldstein G, Holbrook NM (1999) Potential errors in measurement of nonuniform sap flow using heat dissipation probes. *Tree Physiol* 19:681–687
- Dixon MA, Grace J, Tyree MT (1984) Concurrent measurements of stem density, leaf and stem water potential, stomatal conductance, and cavitation on a sapling of *Thuja occidentalis* L. *Plant Cell Environ* 7:615–618
- Goldstein G, Andrade JL, Meinzer FC, Holbrook NM, Cavelier J, Jackson P, Celis A (1998) Stem water storage and diurnal patterns of water use in tropical forest canopy trees. *Plant Cell Environ* 21:397–406
- Granier A (1987) Evaluation of transpiration in a Douglas-fir stand by means of sap flow measurements. *Tree Physiol* 3:309–320
- Hubbard RM, Bond BJ, Ryan MG (1999) Evidence that hydraulic conductance limits photosynthesis in old *Pinus ponderosa* trees. *Tree Physiol* 19:165–172
- Jarvis PG, McNaughton KG (1986) Stomatal control of transpiration: scaling up from leaf to region. *Adv Ecol Res* 15:1–49
- Lloyd J, Grace J, Miranda AC, Meir P, Wong SC, Miranda HS, Wright IR, Gash JHC, McIntyre J (1995) A simple calibrated model of Amazon rainforest productivity based on leaf biochemical properties. *Plant Cell Environ* 18:1129–1145
- LoGullo MA, Salleo S (1992) Water storage in the wood and xylem cavitation in 1-year-old twigs of *Populus deltoides* Bart. *Plant Cell Environ* 15:431–438
- Martin P (1989) The significance of radiative coupling between vegetation and the atmosphere. *Agric For Meteorol* 49:45–53
- Meinzer FC, Grantz DA (1990) Stomatal and hydraulic conductance in rowing sugarcane: stomatal adjustment to water transport capacity. *Plant Cell Environ* 13:383–388
- Meinzer FC, Andrade JL, Goldstein G, Holbrook NM, Cavelier J, Jackson P (1997) Control of transpiration from the upper canopy of a tropical forest: the role of stomatal, boundary layer and hydraulic architecture components. *Plant Cell Environ* 20:1242–1252
- Oberbauer SF, Clark DB, Clark DA, Rich PM, Vega G (1993) Light environment, gas exchange, and annual growth of saplings of three species of rain forest trees in Costa Rica. *J Trop Ecol* 9:511–523
- Pataki D, Oren R, Phillips N (1998) Responses of sap flux and stomatal conductance of *Pinus taeda* L. trees to stepwise reductions in leaf area. *J Exp Bot* 49:871–878
- Phillips N, Bond BJ (1999) A micro-power precision amplifier for converting the output of light sensors to a voltage readable by miniature data loggers. *Tree Physiol* 19:547–549
- Pothier D, Margolis HA, Waring RH (1989) Patterns of change of saturated sapwood permeability and sapwood conductance with stand development. *Can J For Res* 19:432–439
- Ryan MG, Yoder BJ (1997) Hydraulic limits to tree height and tree growth. *BioScience* 47:235–242
- Sperry JS (1995) Limitations on stem water transport and their consequences. In: Gartner BL (ed) *Plant stems: physiology and functional morphology*. Academic, San Diego, pp 105–124
- Sperry JS, Pockman WT (1993) Limitation of transpiration by hydraulic conductance and xylem cavitation in *Betula occidentalis*. *Plant Cell Environ* 16:279–287
- Sperry JS, Alder NN, Eastlack SE (1993) The effect of reduced hydraulic conductance on stomatal conductance and xylem cavitation. *J Exp Bot* 44:1075–1082
- Teskey RO, Hinckley TM, Grier CC (1983) Effect of interruption of flow path on stomatal conductance of *Abies amabilis*. *J Exp Bot* 34:1251–1259
- Tyree MT, Ewers FW (1996) Hydraulic architecture of woody tropical plants. In: Mulkey SS, Chazdon RL, Smith AP (eds) *Tropical forest plant ecophysiology*. Chapman and Hall, New York, pp 217–243
- Whitehead D, Hinckley T (1991) Models of water flux through forest stands: critical leaf and stand parameters. *Tree Physiol* 9:35–57
- Whitehead D, Edwards WRN, Jarvis PG (1984) Conducting sapwood area, foliage area, and permeability in mature trees of *Picea sitchensis* and *Pinus contorta*. *Can J For Res* 14:940–947
- Whitehead D, Livingston NJ, Kelliher FM, Hogan KP, Pepin S, McSeveny TM, Byers JN (1996) Response of transpiration and photosynthesis to a transient change in illuminated foliage for a *Pinus radiata* D. Don tree. *Plant Cell Environ* 19:949–957
- Yoder BJ, Ryan MG, Waring RH, Schoettle AW, Kaufmann MR (1994) Evidence of reduced photosynthetic rates in old trees. *For Sci* 40:513–527
- Zwieniecki MA, Holbrook NM (1998) Diurnal variation in xylem hydraulic conductivity in white ash (*Fraxinus americana* L.), red maple (*Acer rubrum* L.) and red spruce (*Picea rubens* Sarg.) *Plant Cell Environ* 21:1173–1180